REFERENCES

Brett, B.M., (1987). Pollution control in the petrochemicals industry. New York: Lewis Publisher Inc.

Cao, Y., Andretta, A., Heeger, A.J., and Smith, P. (1989). Influence of chemical polymerization conditions on the properties of polyaniline. Polymer, 30, 2305-2312.

Conn, C., Sestak, S., Baker, A.T., and Unsworth, J. (1998). A polyaniline-based selective hydrogen sensors. Electroanalysis, 10(16), 1735-1738.

Dhawan, S.K., Kumar, D., Ram, M.K., Chandra, S., and Trivedi, D.C. (1997). Application of conducting polyaniline as sensor material for ammonia. Sensor and Actuators B, 40, 99-103.

Dyer, A. (1993). An introduction to Zeolite Molecular Sieves. New York: John Wiley.

Frish, H.L. and Mark, J.E. (1996). Nanocomposites prepared by threading polymer chains through zeolites, mesoporous silica or silica nanotubes. Chemistry Material, 8, 1735-1738.

Fukui, K. and Nishida, S. (1997). CO gas sensor based on Au-La$_2$O$_3$ added SnO$_2$ ceramics with siliceous zeolite coat. Sensors and Actuators B, 45, 101-106.

Geng, Y., Li, J., and Jing, X. (1997). Polyaniline doped with macromolecular acids. Synthetic Metals, 84, 81-82.

Goursot, A., Vasilyev, V., and Arbunznikov, A. (1997). Modeling of adsorption properties of zeolites: correlation with the structure. Journal of Physical Chemistry B, 101, 6420-6428.

Huang, W.S., Humphrey, B.D., and MacDiaramid, A.G. (1986). Polyaniline, a novel conducting polymer. Journal of Chemical Society Faraday Translation, 82, 2385-2400.

Jiakun, W. and Hirata, M. (1993). Research into normal temperature gas-sensitive characteristics of polyaniline material. Sensors and Actuator B, 12, 11-13.

Kang, E.T., Neoh, K.G., and Tan, K.L. (1995). Protonation and deprotonation of polyaniline films and powders revisited. Synthetic Metals, 68, 141-144.

Kern, W., Ed. (1993). Handbook of Semicaonductor Cleaning Technology, New Jersey: Noyes Publishing.

Lee, H.K., Shim, M.J., Lee, J.S., and Kim, S.W. (1996). Materials science communication: characteristics of CO gas adsorption on modified natural zeolite. Materials Chemistry and Physics, 44, 79-84.

Li, D., Jiang, Y., Wu, Z., Chen, X., and Li, Y. (2000). Self-assembly of polyaniline ultrathin films based on doping-induced deposition effect and applications for chemical sensors. Sensors and Actuators B, 66, 125-127.

Li, W and Wan, M. (1999). Stability of polyaniline synthesized by a doping-dedoping-redoping method. Journal of Applied Polymer Science, 71, 615.

Limtrakul, J., Khongpracha, P., Jungsuttiwong, S., and Truong, T. (2000). Adsorption of carbon monoxide in H-ZSM-5 and Li-ZSM-5 zeolites: an embedded cluster study. Journal of Molecular Catalysis A: Chemical, 153, 155-163.

MacDiarmid, A.G., Chiang, J.C., and Halpern, M. (1985a). "Polyaniline": Interconversion of metallic and insulating forms. Molecular Crystal Liquid Crystal, 121, 173-180.

MacDiarmid, A.G., Chiang, J.C., and Halpern, M. (1985b). Electrochemical characteristics of "polyaniline" cathodes and anodes in aqueous electrolytes. Molecular Crystal Liquid Crystal, 121, 187-190.

Miasik, J.J., Hooper, A., and Tofield, B.C. (1986). Conducting polymer gas sensor. Journal of Chemical Society Faraday Translation I, 82, 1117-1126

Palaniappan, S. and Narayana, B.H. (1994). Temperature effect on conducting polyaniline salts: thermal and spectral studies. Journal of Polymer Science: Part A: Polymer Chemistry, 32, 2431-2436.

Prissanaroon, W., Ruangchuay, L., Sirivat, A., and Schwank, J. (2000). Electrical conductivity response of dodecylbenzene sulfonic acid-doped polypyrrole films to SO_2-N_2 mixture. Synthetic Metals, 114, 65-72.

Salaneck, W.R., Luncstrom, I., and Ranby, B. (1993). Conjugated Polymer and Related Materials: The Interconnection of Chemical and Electronic Structure. New York: Oxford Science Publications.

Stejskal, J. and Kratochvil, P. (1996). The formation of polyaniline and the nature of its structures. Polymer, 37(2), 367-369.

Wu, C.G. and Bein, T. (1994). Conducting polyaniline filaments in mesoporous channel host. Science, 264, 1757-1759.

Yin, W. and Ruckenstein, E. (2000). Soluble polyaniline co-doped with dodecyl benzene sulfonic acid and hydrochloric acid. Synthetic Metals, 108, 39-46.

Zeng, X.R. and Ko, T.M. (1998). Structure and properties of chemically reduced polyaniline. Polymer, 39(5), 1187-1195.

Zhang, W. and MacDiaramid, A.G. (1995). Conformation effect in doped polyaniline: protonation of amine and imine sites vs. protonation of only imine sites. Polymer Preprints, 26(2), 73-74.

APPENDIX A

FT-IR Spectrum of Emeradine Base and Doped Polyaniline

The polyaniline was first characterised by FT-IR spectroscopy in order to identify functional groups. Ten-mg sample was grounded and mixed with 50-mg KBr. The FT-IR spectrum was observed by using an FT-IR spectrometer (Bruker, model EQUINOX55/S) with the absorption mode 32 scans at the resolution of $4cm^{-1}$.
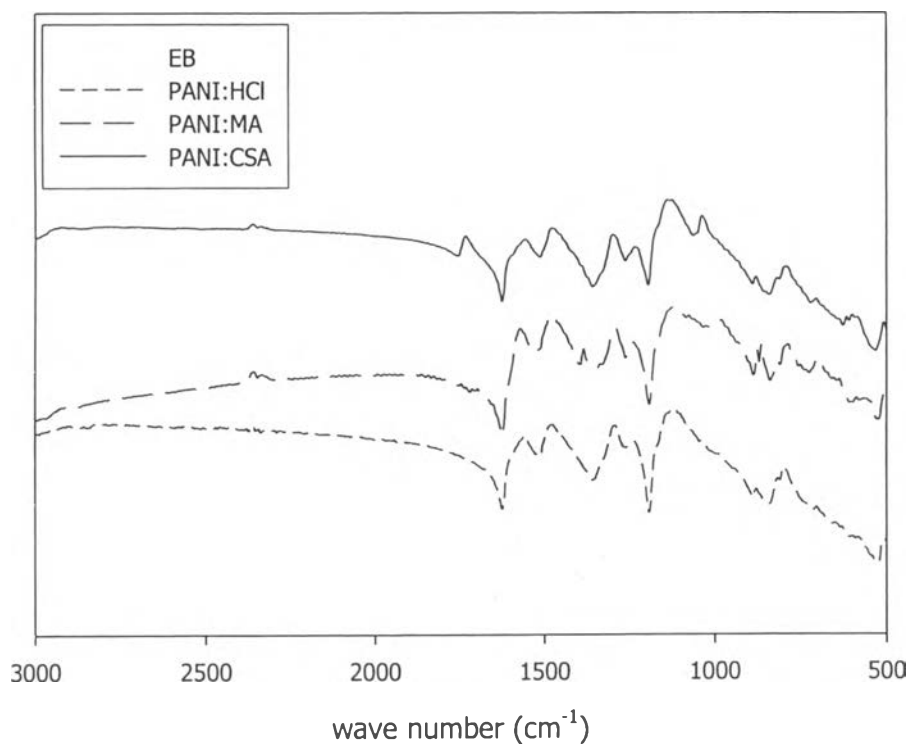

Figure A1 The FT-IR spectrum of PANI doped with HCl, MA, and CSA with $N_A/N_{EB}= 10$.

Table A1 The FT-IR absorption spectrum of polyaniline and doped polyaniline with HCl, MA, and CSA

Absorption mode	Wave number (cm^{-1})				References
	EB	PANI-HCl	PANI-MA	PANI-CSA	
N-H stretching	3242± 3	-	-	3234±2	Kang et al.(1998)
Stretching of C=O group of acid	-	-	1705	1732±3	The Aldrich libraly of FT_IR spectra
Stretching of C=N quinoid ring	1584±2 [1586]	1593 [1564]	1556	1557±6	Zeng and Ko.,(1998)
Stretching of C=C benzenoid ring	1493±2 [1493]	1493 [1484]	1496	1480±1	Zeng and Ko.,(1998)
Stretching of C-N bnzenoid ring	1297±4 [1297]	1302 [1298]	1303	1300±2	Zeng and Ko.,(1998)
Vibration mode of quinoid structure	1155±5 [1161]	1155 [1150]	1223	-	Zeng and Ko.,(1998)
A mode of Q=N+H-B or B-NH_B	-	-	-	1145±7	Morales et al.,(1997)
The sulfonic acid salt group	-	-	-	1035±6	Aldrich library of FT-IR spectra
Out of plan bending of 1,4-ring	824±3 [825]	824 [804]	866	-	Zeng and Ko.,(1998)
Out of plan bending of 1,2-ring	-	-	-	779±5	Kang et al.,(1998)

APPENDIX B

TGA Thermogram of Emeradine Base and Doped Polyaniline

The thermogravimetric analyzer (DuPont, model TGA 2950) was used to determine the amount of moisture content, and dopant in each sample. The experiment was carried out by weighting powder sample of 10-15 mg and placed it in an aluminum pan, and then heated it under a nitrogen gas flow with the heating rate 10 $^{\circ}$C / min from room temperature to 700 $^{\circ}$C. Two transitions were observed in each sample, 110-130 $^{\circ}$C and 130-400 $^{\circ}$C; they refer to the losses of water and dopant, respectively. The degradation temperature of polyaniline appears at 640-670 $^{\circ}$C.

Table B1 The percent weight loss of emeradine base and doped polyaniline

| Sample	Transition temperature ($^{\circ}$C)			% weight loss			% residue
	1st	2nd	3rd	1st	2nd	3rd	
EB	30-120	120-300	300-645	3.69	1.65	24.01	70.65
PANI-1HCl	30-130	130-300	300-645	8.42	9.53	15.01	67.04
PANI-10HCl	30-130	130-300	300-645	11.37	8.80	27.83	51.80
PANI-1MA	30-130	130-300	300-645	7.49	20.18	12.83	59.50
PANI-10MA	30-130	130-300	300-645	5.88	26.98	32.48	34.66
PANI-1CSA	475-670	130-475	475-670	5.31	30.23	29.80	34.66
PANI-10CSA	475-670	130-475	475-670	5.88	34.61	9.08	50.43
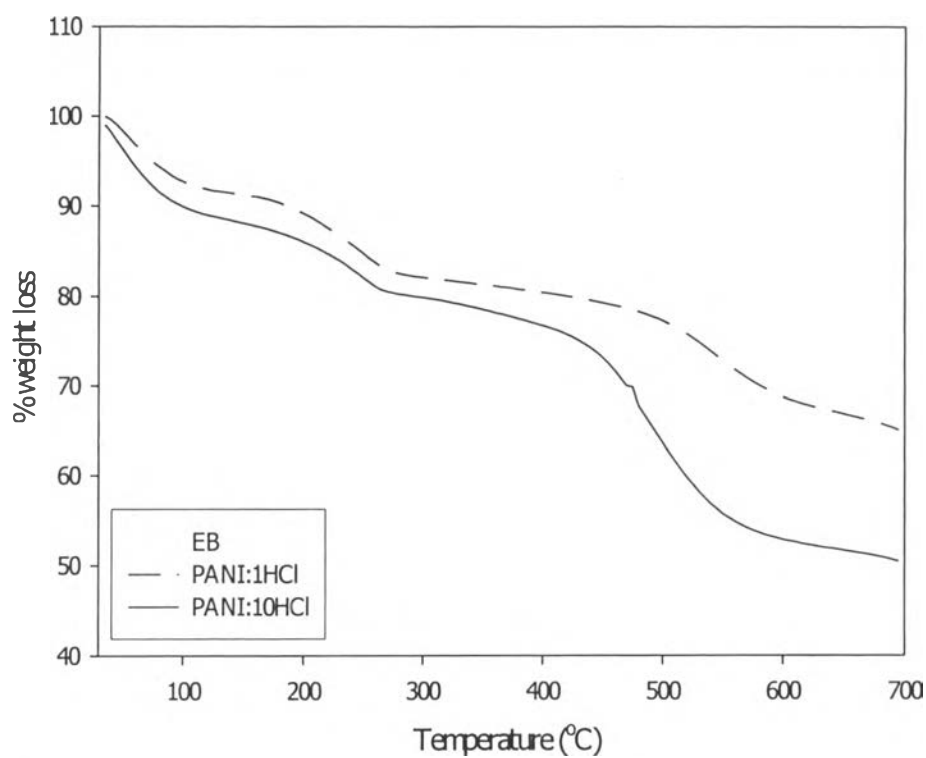
Figure B1 The TGA thermogram of polyaniline doped with HCl.
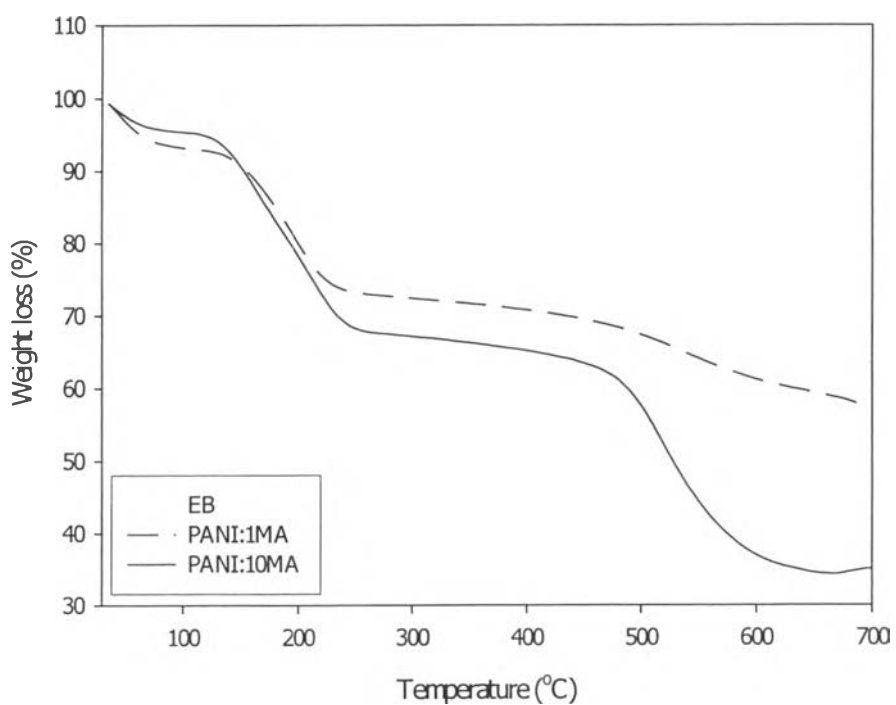

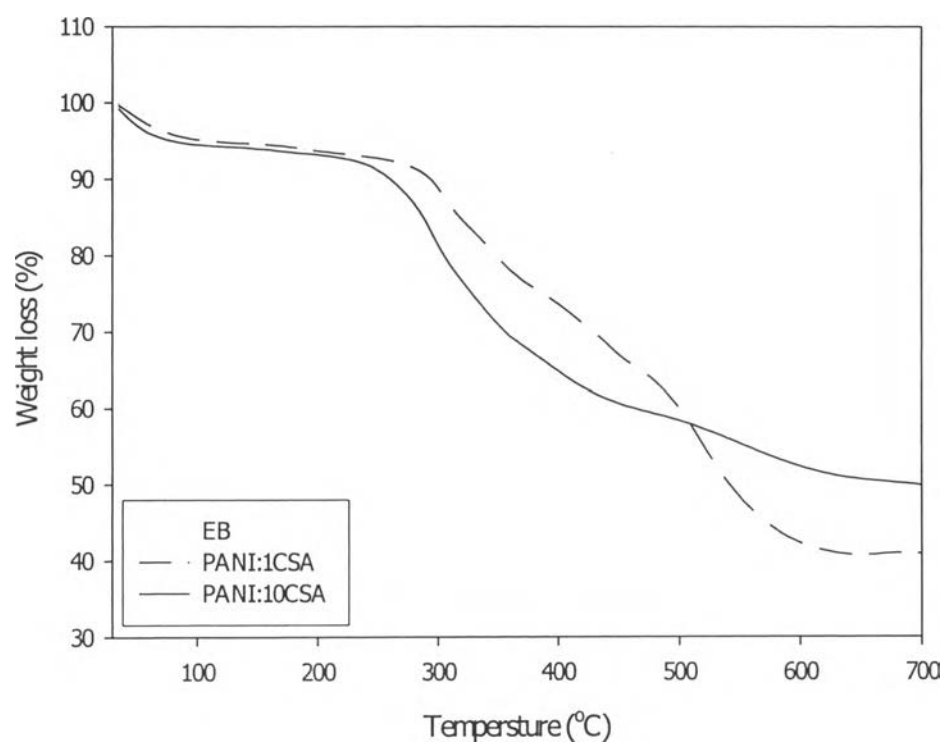**Figure B2** The TGA thermogram of polyaniline doped with MA.

Figure B3 The TGA thermogram of polyaniline dopAed with CSA.

APPENDIX C

Percent Doping Level of Doped Polyaniline Using FT-IR Measurement

The percent doping level of polyaniline can be calculated from the amount of C=C from bezenoid part and the –N= of quinoid part, which was observed from FT-IR spectrum at the wave numbers of 1450 cm^{-1} and 1557 cm^{-1} respectively. The absorbency of each peak was calculated according to Beer's Lambert equation;

$$\text{Beer's law} \qquad A = \varepsilon bc \qquad (C.1)$$

where   A is the area of each peak

      ε is the absorptivity (cm^2/g)

      b is path length (cm)

      c is the concentration of sample (g/cm^3)

The doping ratio of polyaniline can be written following the Beer's law

$$\frac{C_{(C=C)}}{C_{(-N=)}} = \frac{A_{(C=C)}}{A_{(-N=)}} \cdot \frac{\varepsilon_{(-N=)}}{\varepsilon_{(C=C)}} \cdot \frac{b_{(-N=)}}{b_{(C=C)}} \qquad (C.2)$$

By considering the structure of polyaniline, the values of $\frac{C_{(C=C)}}{C_{(-N=)}}$ of fully doped polyaniline and emeradine base are supposed to be equal to 12 and 5.5 respectively. The term $\frac{\varepsilon_{(-N=)}}{\varepsilon_{(C=C)}} \cdot \frac{b_{(-N=)}}{b_{(C=C)}}$ is constant with the same dopant type, which is equal to r. The constant (r) was obtained from the experiment, which are 0.34, 0.20, and 0.18 for PANI doped with HCl, MA, and CSA respectively.

The area of absorption peak was determined by using Gaussian equation.

$$\text{Gaussian equation} = (1/(SD*((2*(22/7))^{0.5})))*\exp(0.5(((x-avg)/SD)^2))*area \qquad (C.3)$$

Finally, the percent doping level of doped polyaniline was calculated by this equation.

$$\% \text{ doping level} = \frac{((A_{(C=C)}/A_{(-N=)})\ r) - 5.5}{12 - 5.5}\ 100 \qquad (C.4)$$

Table C1 Summary of the percent doping level of PANI-HCl, PANI-MA, and PANI-CSA

Sample	Absorption		$A_{(C=C)}/A_{(-N=)}$	% doping level
	$A_{(C=C),1480}$	$A_{(-N=),1557}$		
EB	33.92	66.08	0.51	0.55
1HCl	73.96	26.04	2.84	42.95
10HCl	80.43	19.57	4.11	100.00
1MA	69.53	30.47	2.28	86.70
10MA	71.09	28.91	2.46	100.00
1CSA	65.88	34.12	1.93	77.34
10CSA	68.76	31.24	2.20	100.00

APPENDIX D

Calculation of Doping Level Using Elemental Analysis

The elemental analyzer was used to determine the percents of carbon (%C), hydrogen (%H) and nitrogen (%N) in PANI and doped PANI. The percent doping level was calculated from the ratio of acid per nitrogen in sample. From the weight loss of water from TGA data, the amount of oxygen in PANI sample can be calculated.

$$\% \; O_{water} = \frac{\% \; \text{weight lost of water from TGA x 16 g of O/ mol}}{18 \; g \; H_2O/ \; mol} \qquad (D.1)$$

In addition, the amount of the remaining oxidant has to be subtracted for each sample, before calculating the percent doping level. The calculation of the percent of doping level of emeradine base is by the following equation:

$$\% \; \text{Residue oxidant} = 100 - (\%C + \%H + \%N + \% \; O_{water}) \qquad (D.2)$$

The amount of acid dopant in sample were calculated from the following equation.

$$\% \; \text{element} \; X = 100 - (\%C + \%H + \%N + \% \; O_{water} + \% \; \text{Oxidant}) \qquad (D.3)$$

$$\% \; \text{Appearance doping level} = \frac{\% \; \text{Other element}/14 \; g \; of \; N \; x \; 100}{\% \; N \; x \; (\text{atomic mass of } X)} \qquad (D.4)$$

where   X =   a residue element; in this work, X is referred to Cl for PANI-HCl, 4-atom O for PANI-MA, and 4-atom O and 1-atom S for PANI-CSA.

Table D1 Calculation of doping level from elemental analysis

Sample	Raw data			% water TGA	% O water	%Oxidant (SO_4^-)	%Apparent doping level	% doping level
	%C	%H	%N					
EB	74.251	4.734	14.789	3.69	3.28	2.95	-	-
1HCl	61.542	4.279	11.797	9.02	8.018	2.95	38.17	76.34
10HCl	59.784	4.919	11.404	10.15	9.022	2.95	41.24	82.48
1MA	62.978	4.135	10.512	7.49	6.658	2.95	26.58	53.15
10MA	61.018	3.959	8.748	5.88	5.227	2.95	45.27	90.53
1CSA	62.761	5.825	8.429	5.31	4.72	2.95	26.5	53.01
10CSA	59.834	5.875	6.614	5.88	5.227	2.95	43.01	86.01

The actual doping level is twice of the apparent doping level. So the relative percent doping level can be summarized in Table D1.

Table D2 Raw data from elemental analysis

Sample	% C			% H			% N		
	1	2	Ave.	1	2	Ave.	1	2	Ave.
EB	74.342	74.159	74.251	4.838	4.630	4.734	14.920	14.658	14.489
1HCl	61.757	61.326	61.542	4.430	4.127	4.279	11.908	11.686	11.797
10HCl	59.873	59.695	59.784	5.044	4.794	4.919	11.540	11.268	11.404
1MA	63.004	62.951	62.978	4.265	4.005	4.135	10.643	10.380	10.512
10MA	61.198	60.569	61.018	3.839	4.078	3.959	8.898	8.598	8.748
1CSA	62.952	62.569	62.761	5.929	5.721	5.825	8.891	8.267	8.429
10CSA	59.896	59.772	59.834	5.909	5.840	5.875	6.708	6.519	6.614

APPENDIX E

Determination of the Crystallinity of PANI and Doped PANI

XRD technique was used to investigate the order and the degree of crystallinity of polyanilines. The diffraction patterns of the emeraldine base were typical of an amorphous polymer. On the other hand, all protonic acid doped polyanilines were semi-crystalline polymers. They were identified as follow: the crystalline one corresponds to a relative sharp peak, and the amorphous one is visible as a broad pattern (Lunzy and Banka, 2000). The percentage of crystallinity was determined by integrating area under assumed Guassian curves. Quantitatively, the percentage of crystallinity was calculated from the ratio of the integrated crystalline component intensity to the integrated total intensity.

$$\% \text{ Crystallinity} = \frac{A_{cryst}}{A_{cryst} + A_{amorphous}} \times 100 \qquad (E.1)$$

Where A_{cryst} = The area of crystalline peak

$A_{amorphous}$ = The area of amorphous peak %Crystallinity

Table E1 Values of 2θ, d-spacing ($\overset{o}{A}$) and Miller indices of emeraldine hydrochloride

2θ	d-spacing ($\overset{o}{A}$)	Miller indices
9.5 ± 0.5 [9.5]	9.57	0 0 1
14 ± 1 [14.52]	5.94	0 1 0
20.5 [20.62]	4.26	1 0 0
25.5 ± 2 [25.51]	3.51	1 1 0
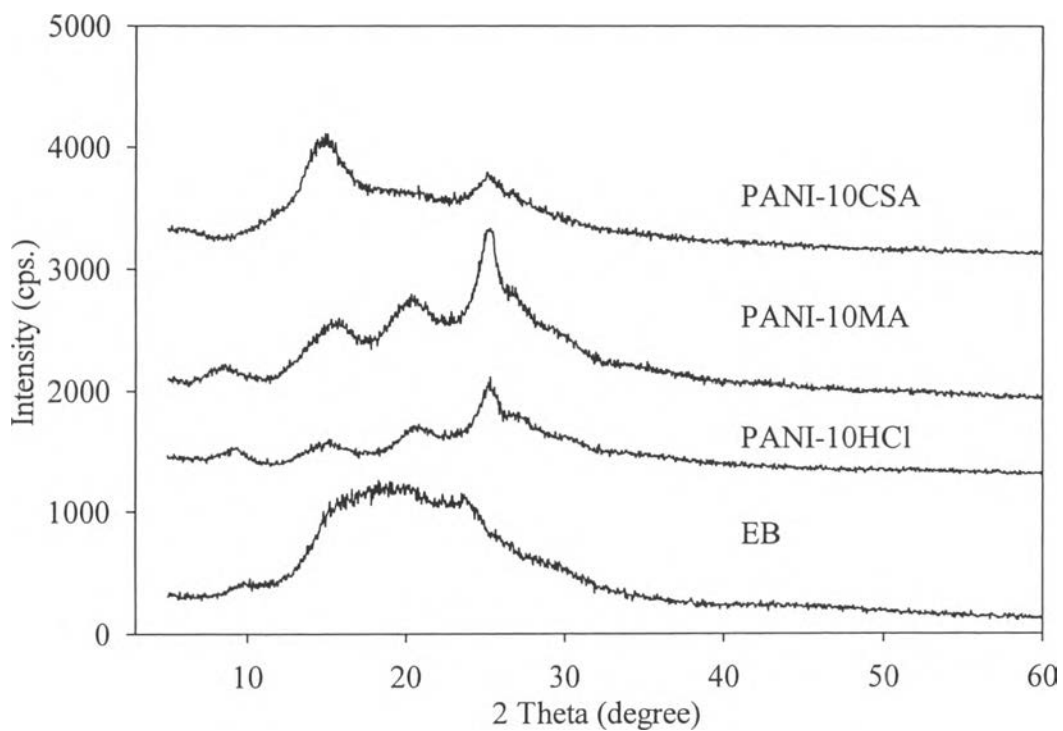
Figure E1 X-ray pattern of PANI and doped PANI with N_A/N_{EB} = 10.

Table E2 Calculated crystallinity of PANI and doped PANI with HCl, MA, and CSA

Sample	% Amorphous	% Crystalline
EB	87.32 ± 2.66	12.68 ± 2.66
PANI-1HCl	70.85 ± 3.36	29.15 ± 3.36
PANI-10HCl	59.23 ± 7.96	40.77 ± 7.96
PANI-1MA	65.85 ± 1.29	34.15 ± 1.29
PANI-10MA	37.10 ± 3.32	62.90 ± 3.32
PANI-1CSA	58.31 ± 2.40	41.69 ± 2.40
PANI-10CSAl	40.50 ± 0.82	59.50 ± 0.82

Characterization of AlMCM41 and Zeolite Y and 13X Using X-ray Diffraction
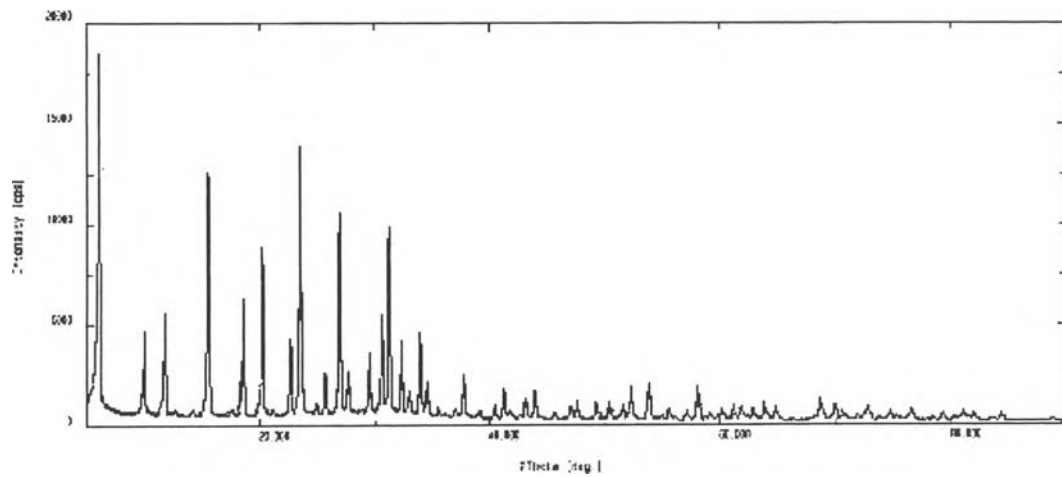
Figure F1 XRD pattern of Cu^{2+}-zeolite Y.
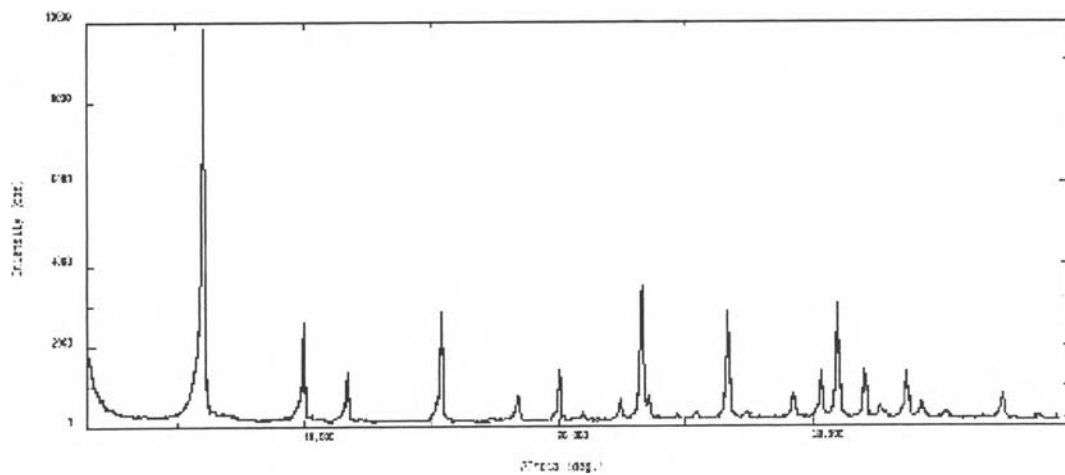
Figure F2 XRD pattern of Cu^{2+}zeolite 13X.

The XRD pattern of AlMCM41 was obtained by scanning the angle between $2\theta = 2\text{-}8°$. The major peaks of AlMCM41, consisting of one intense line and two weak lines, can be indexed to (100), (110), and (300) diffraction lines characteristic of hexagonal structure of MCM41 (Ryoo *et al.*,1997).
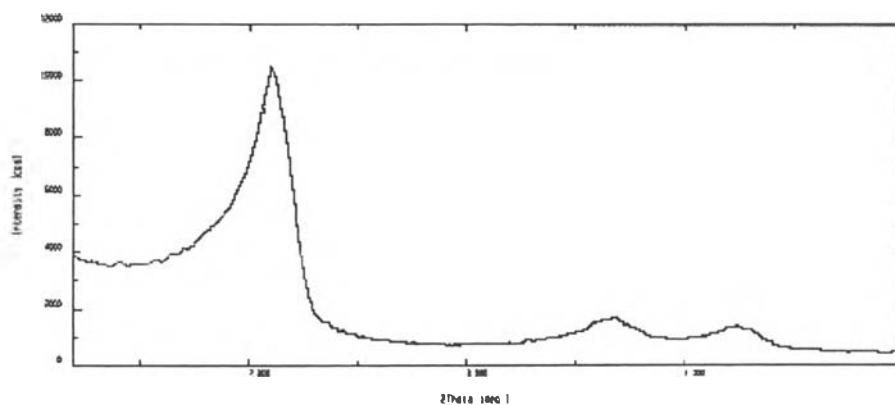
Figure F3 XRD pattern of Cu^{2+}zeolite AlMCM41.

APPENDIX G

Determination of the Cu^{2+} Exchange Capacity of Zeolite Y, 13X, and AlMCM41 Using X-ray Fluorescence

The Cu^{2+} exchange capacities in zeolite Y, 13X, and AlMCM41 were calculated from X-ray Fluorescence data followed by equation G1

$$Cu^{2+} \text{ Exchange capacity} = \frac{(Cu^{2+}_{after} - Cu^{2+}_{before})}{2+} \tag{G.1}$$

Table G1 The element content in Zeolite Y, 13X, and AlMCM41 determined by using X-ray Fluorescence

Sample	Element (%wt)				Si/Al	Cu^{2+} Exchange capacity (mol/gram)
	Si	Al	Na	Cu^{2+}		
Y	68.30	23.90	7.48	0.21	2.86	-
Cu(II)Y	60.60	22.40	6.71	10.20	2.71	0.16
13X	35.20	26.40	38.10	0.14	1.33	-
Cu(II)13X	33.40	26.00	34.40	5.50	1.28	0.08
MCM41	87.60	3.04	7.88	0.28	28.82	-
Cu(II)MCM41	89.10	3.07	4.85	2.79	29.02	0.04

APPENDIX H

Determination of Pore Size and Surface Area of AlMCM41 and Zeolite Y and 13X Using BET

Table H1 Area-volume-pore size summary

	Zeolite Y	Zeolite 13X	AlMCM41
Surface area (m^2/g)	6.92E+02	6.88E+02	5.04E+02
Total pore volume (cc/g)	3.96E-01	4.16E-01	4.54E-01
Average pore diameter (A)	2.29E+01	2.42E+01	3.60E+01

Determination of particle sizes of Y, 13X and AlMCM41 Zeolites by Particle Size Analyzer

Table I1 Summarized the particle diameter and specific surface area of PANI, doped-PANI, Zeolite Y, 13X and Al MCM41

| Sample	Particle diameter (μm)					Specific surface area (sq.m/g)				
	1	2	3	Avg	STD	1	2	3	Avg	STD
EB	32.36	32.19	34.56	33.04	1.32	0.3749	0.3864	0.3837	0.3817	0.01
PANI-1HCl	36.22	22.18	19.96	26.12	8.82	0.4751	0.5541	0.5650	0.5314	0.05
PANI-10HCl	15.1	14.06	13.58	14.25	0.78	0.6658	0.6871	0.7002	0.6844	0.02
PANI-1MA	31.84	31.25	35.56	32.88	2.34	0.3560	0.3623	0.3436	0.3540	0.01
PANI-10MA	33.14	31.35	31.75	32.08	0.94	0.3490	0.3596	0.3589	0.3558	0.01
PANI-1CSA	32.52	30.71	31.94	31.72	0.92	0.3643	0.3700	0.3714	0.3686	0.00
PANI-10CSA	20.62	19.68	19.33	19.88	0.67	0.5670	0.5870	0.5938	0.5826	0.01
Zeolite Y	5.24	4.96	4.81	5.00	0.22	2.2899	2.4049	2.4799	2.3916	0.10
Zeolite 13X	6.62	6.78	6.72	6.71	0.08	2.0854	2.081	2.0837	2.0834	0.00
AlMCM41	18.98	18.5	18.45	18.64	0.29	0.5659	0.5738	0.5768	0.5722	0.01
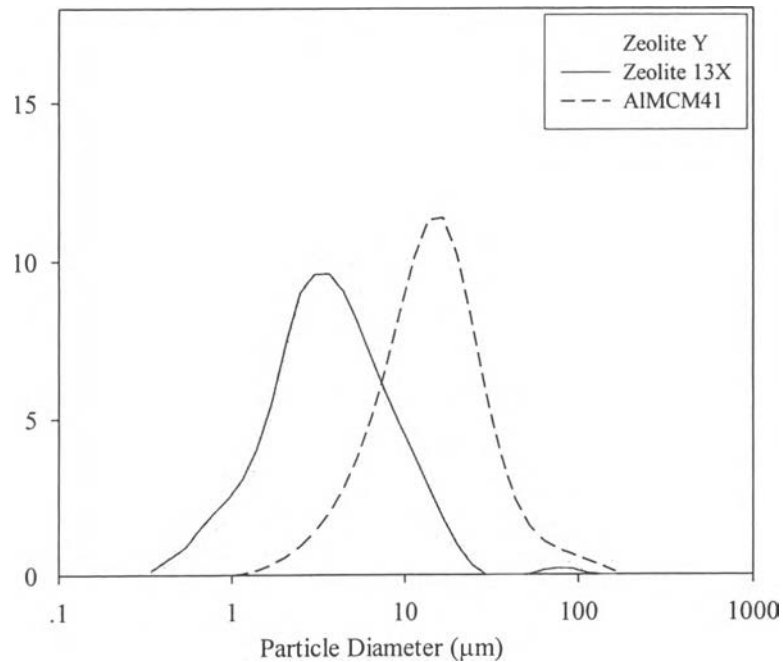
Figure I1 Particle diameters of the Y, 13X and AlMCM41 zeolites.

Table I2 Raw data from particle size analysis of Y zeolite

Size		Zeolite Y					
Low (um)	High (um)	In%	Under %	In%	Under %	In%	Under %
0.20	0.48	0.13	0.14	0.11	0.11	0.10	0.10
0.48	0.59	0.86	1.00	0.88	0.99	0.91	1.01
0.59	0.71	1.47	2.47	1.56	2.55	1.64	2.65
0.71	0.86	1.96	4.43	2.15	4.70	2.29	4.94
0.86	1.04	2.43	6.68	2.74	7.44	2.95	7.89
1.04	1.26	3.05	9.91	3.49	10.93	3.77	11.66
1.26	1.52	4.02	13.93	4.57	15.50	4.91	16.57
1.52	1.84	5.47	19.41	6.10	21.60	6.46	23.03
1.84	2.23	7.37	26.77	7.96	29.56	8.31	31.34
2.23	2.70	9.01	35.78	9.43	38.98	9.68	41.02
2.70	3.27	9.60	45.38	9.78	48.76	9.85	50.87
3.27	3.95	9.61	54.98	9.55	58.31	9.44	60.31
3.95	4.79	9.06	64.04	8.80	67.11	8.56	68.87
4.79	5.79	8.08	72.13	7.70	74.81	7.38	76.25
5.79	7.01	6.96	79.09	6.53	81.34	6.18	82.43
7.01	8.48	5.85	84.93	5.40	86.74	5.07	87.50
8.48	10.27	4.81	89.74	4.39	91.13	4.10	91.60
10.27	12.43	3.81	93.55	3.41	94.54	3.21	94.81
12.43	15.05	2.80	96.36	2.45	96.99	2.32	97.13
15.05	18.21	1.81	98.17	1.52	98.51	1.44	98.57
18.21	22.04	0.94	99.11	0.73	99.24	0.70	99.27
22.04	26.68	0.31	99.42	0.18	99.42	0.18	99.44
26.68	32.29	0.00	99.42	0.00	99.42	0.00	99.44
32.29	39.08	0.00	99.42	0.00	99.42	0.00	99.44
39.08	47.30	0.00	99.42	0.00	99.42	0.00	99.44
47.30	57.25	0.01	99.43	0.01	99.43	0.00	99.44
57.25	69.30	0.14	99.57	0.13	99.56	0.12	99.56
69.30	83.87	0.20	99.77	0.20	99.76	0.19	99.75
83.87	101.52	0.18	99.95	0.18	99.94	0.19	99.94
101.52	122.87	0.05	100.00	0.06	100.00	0.06	100.00
122.87	148.72	0.00	100.00	0.00	100.00	0.00	100.00
148.72	180.00	0.00	100.00	0.00	100.00	0.00	100.00

Table I3 Raw data from particle size analysis of 13X zeolite

Size		13X					
Low (um)	High (um)	In%	Under %	In%	Under %	In%	Under %
0.20	0.48	0.08	0.08	0.08	0.08	0.08	0.08
0.48	0.59	0.56	0.65	0.56	0.64	0.57	0.65
0.59	0.71	0.99	1.63	0.99	1.63	0.99	1.64
0.71	0.86	1.37	3.00	1.37	3.00	1.37	3.01
0.86	1.04	1.81	4.81	1.81	4.81	1.82	4.83
1.04	1.26	2.47	7.28	2.47	7.28	2.48	7.31
1.26	1.52	3.52	10.80	3.52	10.80	3.52	10.83
1.52	1.84	5.05	15.85	5.04	15.84	5.05	15.88
1.84	2.23	6.99	22.84	6.98	22.82	6.99	22.87
2.23	2.70	8.89	31.73	8.86	31.68	8.87	31.74
2.70	3.27	10.16	41.88	10.11	41.79	10.13	41.87
3.27	3.95	10.77	52.65	10.71	52.50	10.73	52.60
3.95	4.79	10.54	63.19	10.46	62.96	10.48	63.08
4.79	5.79	9.40	72.60	9.32	72.28	9.33	72.41
5.79	7.01	7.58	80.16	7.51	79.79	7.51	79.92
7.01	8.48	5.49	85.66	5.45	85.24	5.43	85.35
8.48	10.27	3.61	89.27	3.61	88.85	3.58	88.93
10.27	12.43	2.24	91.51	2.25	91.11	2.24	91.17
12.43	15.05	1.43	92.95	1.46	92.57	1.46	92.63
15.05	18.21	1.06	94.01	1.10	93.67	1.11	93.74
18.21	22.04	0.92	94.92	0.97	94.64	0.99	94.73
22.04	26.68	0.87	95.79	0.93	95.57	0.95	95.68
26.68	32.29	0.83	96.62	0.90	96.47	0.90	96.58
32.29	39.08	0.76	97.38	0.82	97.29	0.81	97.39
39.08	47.30	0.66	98.05	0.69	97.98	0.67	98.06
47.30	57.25	0.57	98.61	0.56	98.54	0.54	98.60
57.25	69.30	0.51	99.13	0.49	99.03	0.47	99.07
69.30	83.87	0.46	99.59	0.46	99.49	0.44	99.51
83.87	101.52	0.35	99.93	0.39	99.88	0.37	99.88
101.52	122.87	0.07	100.00	0.12	100.00	0.12	100.00
122.87	148.72	0.00	100.00	0.00	100.00	0.00	100.00
148.72	180.00	0.00	100.00	0.00	100.00	0.00	100.00

Table I4 Raw data from particle size analysis of AlMCM41 zeolite

Size		MCM41					
Low (um)	High (um)	In%	Under %	In%	Under %	In%	Under %
0.20	0.48	0.00	0.00	0.00	0.00	0.00	0.00
0.48	0.59	0.00	0.00	0.00	0.00	0.00	0.00
0.59	0.71	0.00	0.00	0.00	0.00	0.00	0.00
0.71	0.86	0.00	0.00	0.00	0.00	0.00	0.00
0.86	1.04	0.00	0.00	0.00	0.00	0.00	0.00
1.04	1.26	0.03	0.04	0.04	0.04	0.03	0.03
1.26	1.52	0.14	0.18	0.14	0.18	0.14	0.17
1.52	1.84	0.32	0.49	0.31	0.49	0.32	0.49
1.84	2.23	0.57	1.06	0.57	1.06	0.57	1.06
2.23	2.70	0.91	1.98	0.92	1.98	0.91	1.97
2.70	3.27	1.37	3.35	1.38	3.36	1.37	3.34
3.27	3.95	1.97	5.33	1.98	5.34	1.97	5.31
3.95	4.79	2.75	8.11	2.77	8.11	2.75	8.06
4.79	5.79	3.76	11.90	3.80	11.91	3.76	11.81
5.79	7.01	5.05	17.02	5.11	17.02	5.05	16.86
7.01	8.48	6.63	23.73	6.71	23.73	6.63	23.49
8.48	10.27	8.42	32.24	8.51	32.24	8.42	31.91
10.27	12.43	10.13	42.43	10.19	42.43	10.13	42.04
12.43	15.05	11.29	53.74	11.31	53.74	11.29	53.32
15.05	18.21	11.37	65.09	11.35	65.09	11.37	64.69
18.21	22.04	10.19	75.22	10.14	75.23	10.19	74.88
22.04	26.68	8.12	83.28	8.05	83.28	8.12	83.00
26.68	32.29	5.83	89.04	5.77	89.05	5.83	88.83
32.29	39.08	3.87	92.86	3.81	92.86	3.87	92.70
39.08	47.30	2.43	95.25	2.39	95.25	2.43	95.13
47.30	57.25	1.55	96.75	1.50	96.75	1.55	96.68
57.25	69.30	1.07	97.78	1.02	97.77	1.07	97.75
69.30	83.87	0.81	98.52	0.75	98.52	0.81	98.55
83.87	101.52	0.63	99.09	0.57	99.09	0.63	99.18
101.52	122.87	0.45	99.52	0.42	99.52	0.45	99.63
122.87	148.72	0.28	99.82	0.30	99.82	0.28	99.91
148.72	180.00	0.09	100.00	0.18	100.00	0.09	100.00

Scanning Electron Micrograph of PANI, Doped PANI, and Zeolites
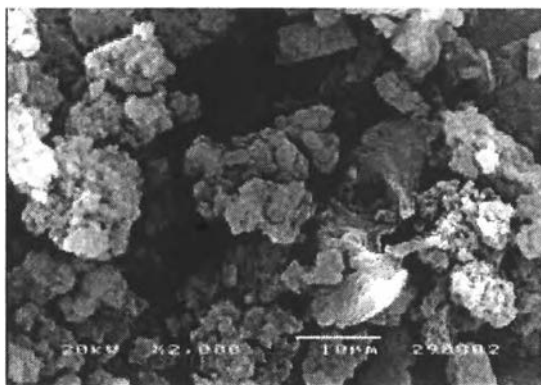

Figure J1 The morphology of polyaniline emeraldine base powder at magnification 2000.
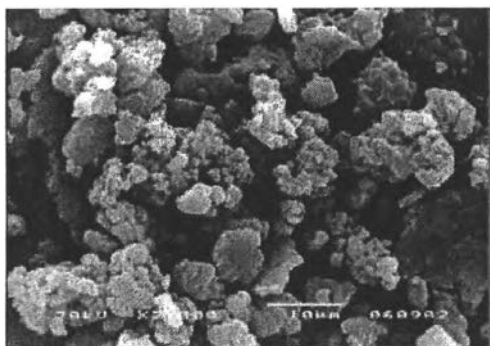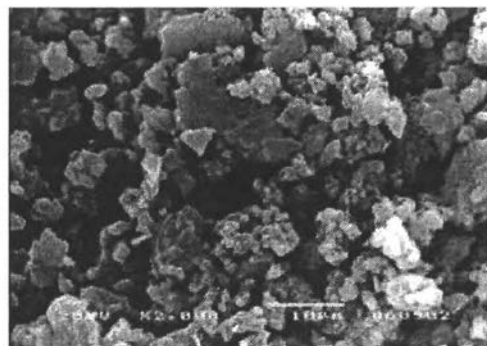
a)   b)

Figure J2 The morphology of polyaniline powder doped with HCl at magnification 2000 a) PANI-1HCl and b) PANI-HCl.
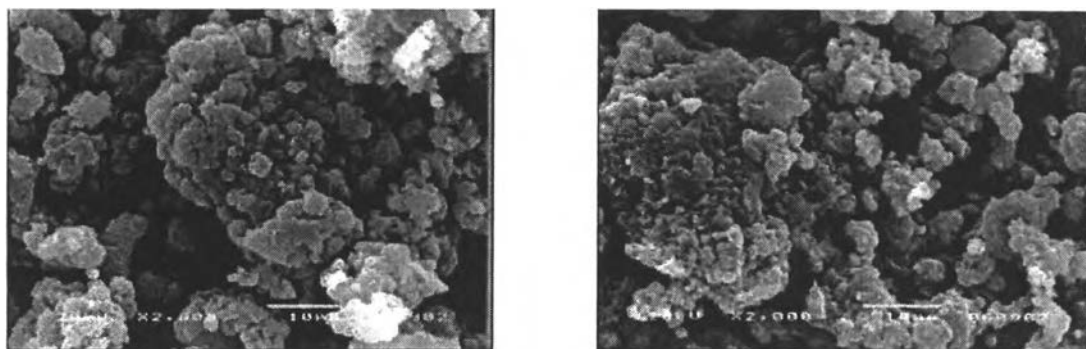
a)

b)

Figure J3 The morphology of polyaniline powder doped with MA at magnification 2000 a) PANI-1MA and b) PANI-MA.
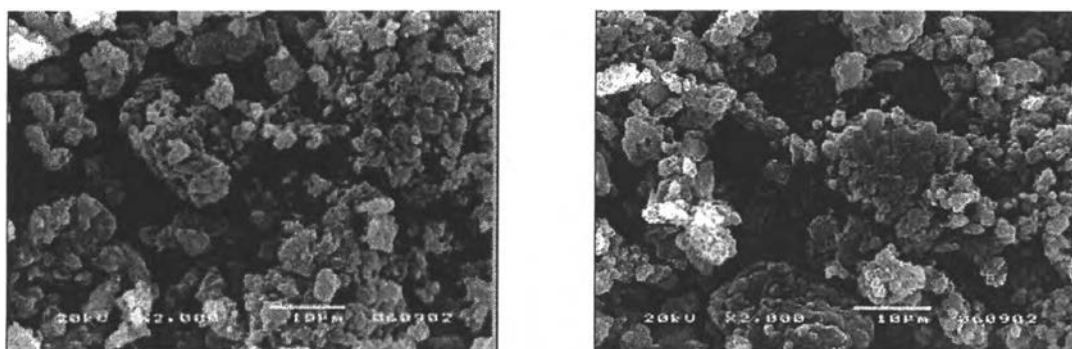
a)

b)

Figure J4 The morphology of polyaniline powder doped with CSA at magnification 2000 a) PANI-1CSA and b) PANI-CSA.
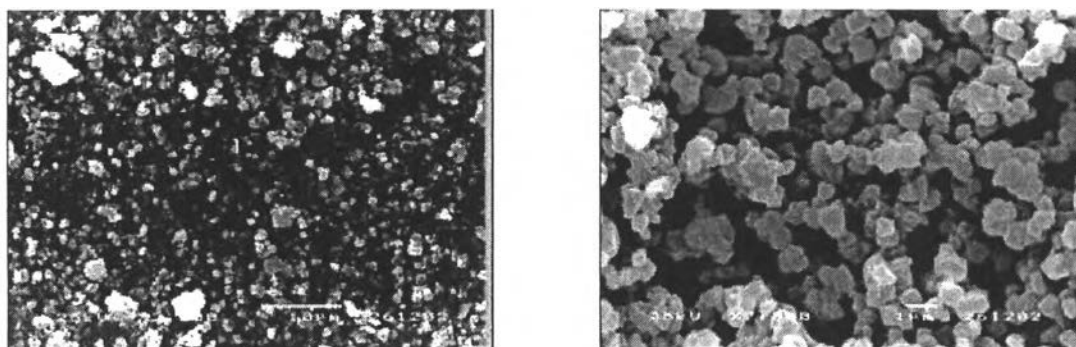
a)   b)

Figure J5 The morphology of Cu^{2+} Zeolite Y powder a) x2000 and b) x7500.
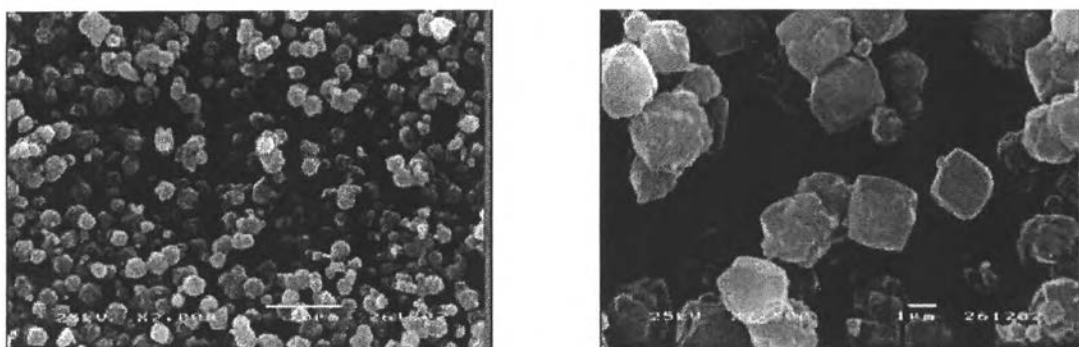
a)   b)

Figure J6 The morphology of Cu^{2+} Zeolite 13X powder a) x2000 and b) x7500.
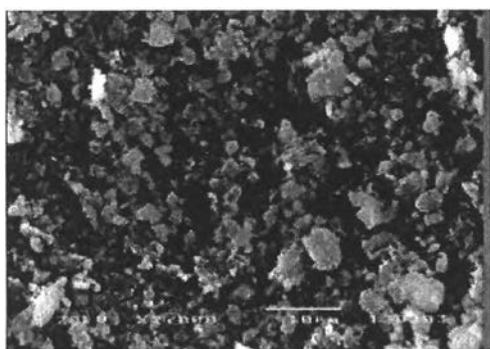
a)
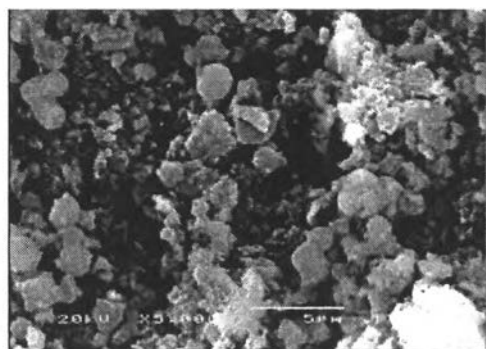
b)
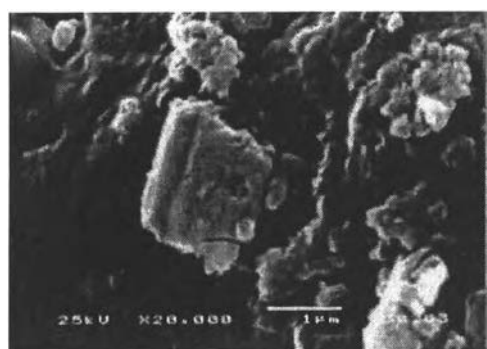
c)

Figure J7 The morphology of Cu^{2+} AlMCM41 powder a) x2000 b) x5000, and c) 20000.
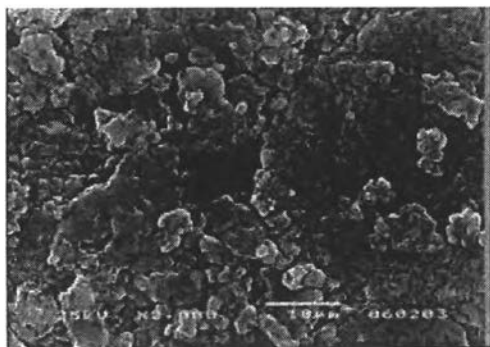
a)
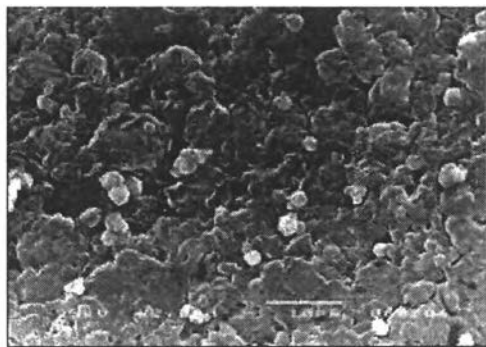
b)
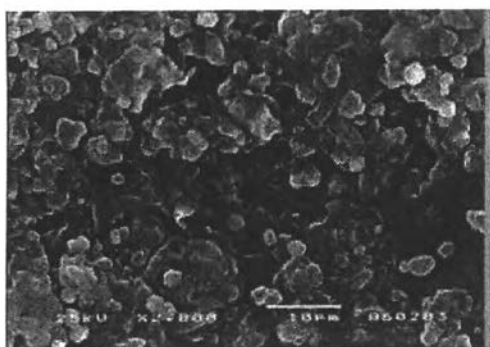
c)
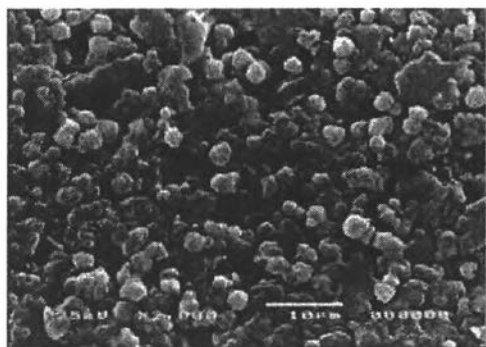
d)

Figure J8 The morphology of PANI and PANI composite with zeolite 13X at magnification 2000 a) PANI-10MA, b) PANI-10MA/10-13X, c) PANI-10MA/20-13X, and d) PANI-10MA/40-13X.
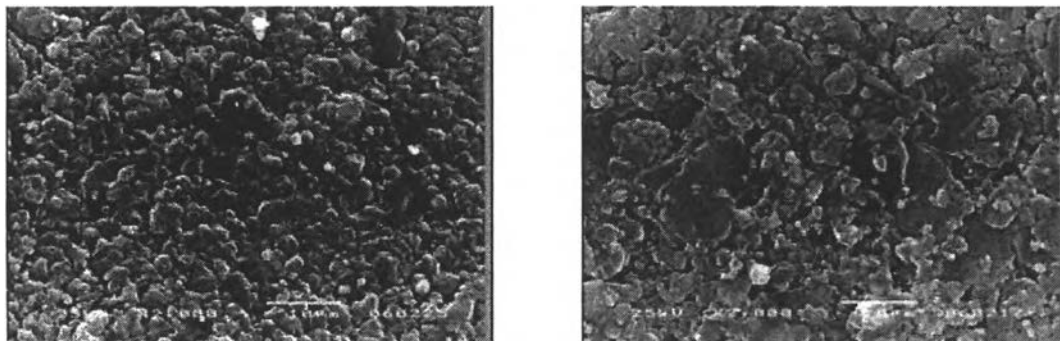
a)   b)

Figure J9 The morphology of PANI composite with zeolite Y and AlMCM41 at magnification 2000 a) PANI-10MA/10-Y and b) PANI-10MA/10-AlMCM41.

APPENDIX K

Determination of the Correction Factor (K)

The electrical conductivity of sample was measured by a four-point probe meter. Probe head assemblies are available in two different arrangements depending on the probe pins; a linear array and a square array. For the linear array, a constant current (I) was applied to the two outer electrodes and the sample voltage (V) was measured between the two inner electrodes as shown in the figure (appendix figure).
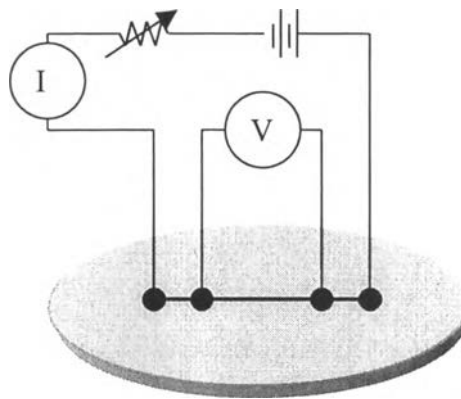
Figure K1 Linear four-point probe array.

The correct factor (K) is used to account the geometrical effects in sheet resistivity measurement of microelectronic structure.

$$K = \frac{w}{l} \qquad \qquad (K.1)$$

where   K   is geometrical correction factor

w   is width of probe tip spacing (cm)

l   is the length between probe (cm)

In this measurement, the constant K value was determined by using a standard sheet with a known resistivity value; we used silicon wafer chips (SiO_2). K was calculated by using Equation K.2.

$$K = \frac{\rho}{R} \frac{1}{t} = \frac{I}{V} \frac{\rho}{t} \qquad \text{(K.2)}$$

where   K   =   geometric correction factor

             ρ =   resistivity of stand materials which were calibrated by using a four point probe at King Mongkut's Institute Technology of Lad Krabang (Ω.cm)

             t   =   film thickness (cm)

             R   =   film resistance (Ω)

             I   =   current (A)

             V   =   voltage drop (V).

Standard Si wafer were cleaned to remove organic impurities prior to be used according to the standard RCA method (Kern, 1993).

Materials

Acetones (CARLO ERBA, 99.8%), Methanol (CARLO ERBA, 99.9%), Ammonium hydroxide (Merck, 99.9%), Hydrogen peroxide (CARLO ERBA, 30% in water), and dilute (2%) Hydrofuric acid

Experiment

The cleaning procedures contain 3 steps, solvent clean, RCA01 and HF dip. The first step is the solvent clean step, employed to remove oils and organic residues that appeared on Si surface. The Si wafer was placed into the acetone at 55 °C (not excess than 55 °C) for 10 min, removed and placed in methanol for 2-5 min, subsequently rinsed with deionised water and blown dried with nitrogen gas. Second step is the RCA clean, to remove organic residues from silicon wafers. This process oxidized the silicon wafer and left a thin oxide on the surface of the wafer. RCA solution was prepared with 5 parts of water (H_2O), 1 part of 27% ammonium hydroxide (NH_4OH), and 1 part of 30% hydrogen peroxide (H_2O_2). 65 ml of NH_4OH

(27%) was added into 325 ml of DI water in a beaker and then heated to 70±5 °C. The mixture would bubble vigorously after 1-2 minutes, indicated that it is ready to use. Silicon wafer was soaked in the solution for 15 min, consequently overflowed with DI water in order to rinse and remove the solution. The third step is HF dip, which was used to remove native silicon dioxide from wafers. 480 ml of DI water was added to the polypropylene bottle and then added 20 ml HF. Wafer was soaked in this solution for 2 min, removed and checked for hydrophobicity by performing the wetting test. DI water was poured onto the surface wafer, the clean silicon surface would show the bead of water roll off. Clean Si wafer was further blown dried with nitrogen and stored in a clean and dry environment.

Table K1 Determination the correction factor of probe A and B

Probe	K (correction factor)				
	1	2	3	Average	SD
A	3.901	3.841	3.871	3.871	0.030
B	3.635	4.013	4.071	3.906	0.237
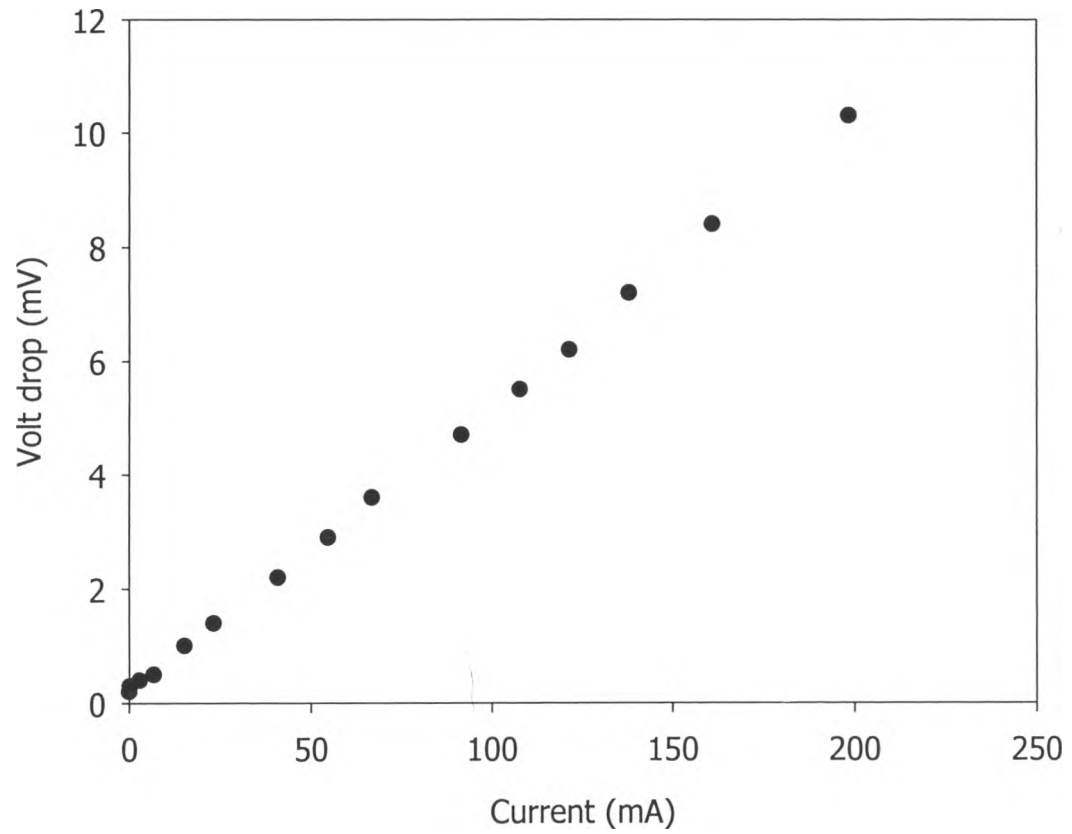
Figure K2 Show the calibration data of Si-wafer: K tay which specific resistivity 0.014265 Ω.cm thickness 0.0724 cm.

Table K2 Determination the correction factor of probe A with standard Si wafer (specific resistivity 0.014265 Ω.cm, thickness 0.0724 cm.)

Volt Applied (V)			Current (mA)			Voltage drop (mV)		
1	2	3	1	2	3	1	2	3
0.003	0.008	0.002	2.80E-03	2.90E-03	2.70E-03	0.2	0.5	0
0.73	1.602	0.376	2.83	3.23	7.26E-02	0.4	0.6	0.10
1.087	3.01	0.779	6.67	7.36	5.06	0.5	0.9	0.40
1.714	3.76	1.324	15.15	17.62	11.40	1.00	1.2	0.70
2.14	3.94	2.02	23.2	33.60	20.80	1.40	2.00	1.20
2.87	3.93	2.48	40.8	43.20	35.00	2.20	2.60	1.90
3.22	4.11	2.85	54.6	59.50	53.60	2.90	3.40	2.80
3.38	3.85	3.16	66.8	78.60	68.40	3.60	4.30	3.60
3.67	4.09	3.80	107.6	101.9	108.4	5.50	5.50	5.60
3.93	4.06	4.06	138.0	131.2	129.9	7.20	7.00	6.70
4.18	4.02	4.12	160.7	167.3	164.6	8.40	8.90	8.50
4.07	4.12	4.50	198.3	194.2	182.2	10.30	10.6	9.40

(Temperature 25°C, Humidity 54%)

Table K3 Determination the correction factor of probe B with standard Si wafer (specific resistivity 0.014265 Ω.cm, thickness 0.0724 cm.)

Volt Applied (V)			Current (mA)			Voltage drop (mV)		
1	2	3	1	2	3	1	2	3
1.88	0.004	0.004	1.95E-02	2.70E-03	3.00E-03	0.9	0.3	0.7
2.35	1.165	0.822	3.50	2.41	4.68	1.20	0.4	0.8
3.26	2.27	1.637	13.47	7.43	16.58	1.70	0.6	1.3
3.55	3.00	2.24	36.20	17.72	32.00	2.60	1.10	2.00
3.88	3.04	2.44	53.50	29.50	43.20	3.50	1.70	2.60
3.91	3.42	2.80	83.20	47.00	60.50	5.40	2.50	3.40
3.69	3.77	3.04	107.3	89.30	82.90	6.80	4.60	4.60
3.8	3.84	3.2	124.5	119.80	115.8	7.60	6.10	6.10
3.92	4.03	3.34	155.5	150.20	138.5	9.20	7.60	7.30
4.05	3.89	3.61	191.7	191.10	182.1	11.30	9.70	9.40

(Temperature 25°C, Humidity 54%)

APPENDIX L

Determination of Ohmic Regime

The Ohmic rigime was defined as the regime which the applied voltage linearly depends on the applied current according to the Ohmic's law.

$$V = IR \qquad (L.1)$$

where V_a = applied voltage (mV)

                I = current   (mA)

                R = resistance   (Ω)
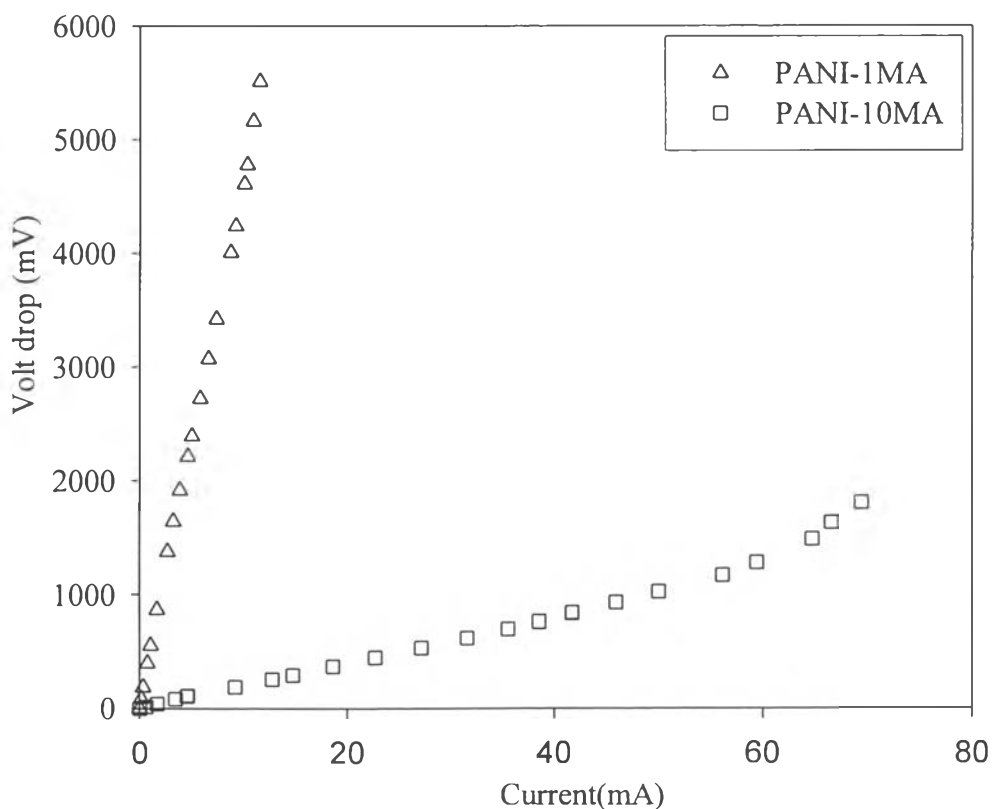
Figure L1 Linear regime of PANI doped maleic acid with N_A/N_{EB} = 1 and 10

Table L1 The raw data of the determiantion of linear regime of doped PANI

Sample	Thickness (mm.)	V applied (V)		I applied (mA)		V drop (mV)		Conductivity (S.cm)	
		1	2	1	2	1	2	1	2
PANI-1HCl	1) 0.1342	0.02	0.90	0.00	0.38	2.60	160.50	2.00E-02	4.41E-02
	2) 0.1384	1.39	2.13	0.27	0.86	242.00	328.00	2.12E-02	4.90E-02
		4.52	3.09	0.90	1.24	800.00	459.00	2.16E-02	5.04E-02
		6.12	4.03	1.24	1.60	1087.00	588.00	2.20E-02	5.09E-02
		10.16	5.32	2.16	2.16	1864.00	787.00	2.23E-02	5.12E-02
		13.64	6.68	2.96	2.68	2440.00	971.00	2.34E-02	5.15E-02
		19.19	8.24	4.23	3.18	3460.00	1143.00	2.35E-02	5.19E-02
		22.90	11.44	5.09	3.90	4180.00	1391.00	2.34E-02	5.23E-02
		27.10	13.29	6.03	3.78	5060.00	1340.00	2.29E-02	5.27E-02
		33.10	15.61	6.54	3.81	6150.00	1342.00	2.05E-02	5.30E-02
		37.20	18.42	6.71	4.03	7610.00	1425.00	1.70E-02	5.28E-02
PANI-10HCl	1) 0.1294	1.40	0.01	8.80	0.00	233.00	0.10	7.54E-01	5.41E-01
	2) 0.1337	2.28	0.42	11.29	1.52	284.00	51.20	7.94E-01	5.74E-01
		3.11	0.86	16.54	4.87	397.00	150.70	8.32E-01	6.24E-01
		4.14	1.67	24.00	10.10	562.00	269.00	8.53E-01	7.25E-01
		5.50	3.12	31.90	18.89	737.00	488.00	8.64E-01	7.48E-01
		6.78	4.14	36.10	27.60	836.00	696.00	8.62E-01	7.66E-01
		10.40	5.09	40.90	34.00	1115.00	846.00	7.32E-01	7.77E-01
		14.17	6.65	38.80	43.30	1113.00	1056.00	6.96E-01	7.92E-01

Table L1 (Continued)

Sample	Thickness (mm.)	V applied (V)		I applied (mA)		V drop (mV)		Conductivity (S.cm)	
		1	2	1	2	1	2	1	2
PANI-1MA	1) 0.1396	0.01	0.02	0.00	0.01	1.80	3.6	3.19E-02	4.13E-02
	2) 0.1199	0.56	0.54	0.15	0.17	87.20	85.4	3.27E-02	4.17E-02
		1.03	1.14	0.34	0.43	188.00	218	3.35E-02	4.23E-02
		2.32	2.18	0.74	0.78	400.00	392	3.42E-02	4.27E-02
		3.25	2.95	1.05	1.05	557.00	526	3.48E-02	4.29E-02
		5.10	4.10	1.66	1.46	865.00	730	3.55E-02	4.31E-02
		7.92	5.55	2.67	2.02	1367.00	1009	3.61E-02	4.31E-02
		9.64	8.28	3.24	3.00	1634.00	1479	3.67E-02	4.37E-02
		11.35	10.87	3.85	3.86	1912.00	1892	3.73E-02	4.40E-02
		13.60	13.92	4.61	4.95	2210.00	2360	3.86E-02	4.52E-02
		14.84	16.63	5.04	5.73	2390.00	2720	3.90E-02	4.54E-02
		16.94	18.69	5.80	6.38	2720.00	3020	3.95E-02	4.55E-02
		19.13	19.58	6.58	6.56	3070.00	3120	3.97E-02	4.53E-02
		21.20	20.70	7.37	6.94	3420.00	3290	3.99E-02	4.54E-02
		25.60	22.90	8.72	7.55	4010.00	3590	4.02E-02	4.53E-02
		27.90	24.40	9.19	7.84	4240.00	3750	4.01E-02	4.50E-02
		31.10	26.70	10.01	8.38	4610.00	4000	4.02E-02	4.51E-02
		33.50	29.20	10.30	8.89	4780.00	4250	3.99E-02	4.51E-02
		37.40	32.10	10.86	9.34	5160.00	4490	3.89E-02	4.48E-02
		40.90	35.20	11.46	9.82	5510.00	4770	3.85E-02	4.44E-02
		43.10	39.00	11.12	10.51	5460.00	5160	3.77E-02	4.39E-02
		46.00	42.90	10.93	11.06	5500.00	5560	3.68E-02	4.29E-02
		49.50	46.00	11.48	11.08	5800.00	5660	3.66E-02	4.22E-02

Table L1 (Continued)

Sample	Thickness (mm.)	V applied (V)		I applied (mA)		V drop (mV)		Conductivity (S.cm)	
		1	2	1	2	1	2	1	2
PANI-10MA	1) 0.1170	1.11	0.99	11.45	9.18	198.00	191.00	1.28E+00	1.09E+00
	2) 0.1141	1.42	1.28	15.10	12.69	254.00	258.00	1.31E+00	1.11E+00
		1.62	1.45	17.40	14.69	288.00	295.00	1.33E+00	1.13E+00
		1.84	1.82	19.84	18.60	326.00	371.00	1.34E+00	1.14E+00
		2.12	2.16	23.80	22.70	385.00	451.00	1.36E+00	1.14E+00
		2.62	2.58	29.90	27.10	478.00	534.00	1.38E+00	1.15E+00
		2.93	3.01	32.20	31.50	512.00	620.00	1.39E+00	1.15E+00
		3.34	3.40	36.30	35.50	575.00	699.00	1.39E+00	1.15E+00
		3.78	3.73	40.40	38.50	640.00	762.00	1.39E+00	1.14E+00
		4.63	4.18	47.70	41.70	759.00	837.00	1.39E+00	1.13E+00
		5.41	4.69	51.90	45.90	838.00	926.00	1.37E+00	1.12E+00
		6.30	5.25	54.10	50.00	898.00	1019.00	1.33E+00	1.11E+00
		7.41	6.19	56.60	56.10	966.00	1163.00	1.29E+00	1.09E+00
		8.71	7.19	59.90	59.40	1055.00	1272.00	1.25E+00	1.06E+00
PANI-1CSA	1) 0.1193	2.87	2.53	1.22	1.295	450	377	5.87E-02	7.17E-02
	2) 0.1238	4.33	3.31	1.98	1.745	715.00	507	5.99E-02	7.18E-02
		4.88	3.92	2.41	2.13	858	614	6.08E-02	7.24E-02
		6.97	4.89	3.65	2.63	1266	757	6.24E-02	7.25E-02
		7.54	6.68	4.04	3.61	1384	1037	6.32E-02	7.26E-02
		9.57	8.2	5.25	4.5	1779	1281	6.39E-02	7.33E-02
		10.25	10.06	5.68	5.54	1900	1572	6.47E-02	7.35E-02
		13.25	10.9	7.58	6.04	2450	1708	6.70E-02	7.38E-02
		15.06	12.15	8.79	6.78	2785	1915	6.83E-02	7.39E-02
		16.69	14	9.67	7.85	3070	2160	6.82E-02	7.58E-02
		18.49	15.09	10.67	8.52	3370	2340	6.86E-02	7.60E-02
		20	16.96	11.56	9.6	3630	2630	6.90E-02	7.62E-02
		22.3	19.5	12.6	11.16	3940	3040	6.92E-02	7.66E-02

Table L1 (Continued)

Sample	Thickness (mm.)	V applied (V)		I applied (mA)		V drop (mV)		Conductivity (S.cm)	
		1	2	1	2	1	2	1	2
		24.1	20.4	13.04	11.78	4080	3220	6.92E-02	7.63E-02
		26.9	22.2	13.81	12.84	4320	3500	6.92E-02	7.65E-02
		28.6	24.2	14.18	13.8	4440	3770	6.92E-02	7.64E-02
		30.30	26.3	14.84	14.93	4640.00	4070	6.93E-02	7.65E-02
		32.30	28.7	15.62	16.02	4890.00	4380	6.92E-02	7.63E-02
		34.40	30	16.58	16.68	5170.00	4570	6.94E-02	7.62E-02
		36.20	33.3	17.08	18.46	5340.00	5060	6.93E-02	7.61E-02
		38.60	34.3	16.69	18.58	5300.00	5170	6.82E-02	7.50E-02
PANI-1CSA	1) 0.1148 2) 0.1087	1.56	1.178	25.40	17.48	268.00	235.00	2.13E+00	1.55E+00
		1.81	1.3	29.40	21.50	307.00	289.00	2.15E+00	1.55E+00
		2.18	1.693	34.00	28.30	352.00	378.00	2.17E+00	1.56E+00
		2.84	1.875	44.90	31.60	456.00	421.00	2.22E+00	1.57E+00
		3.34	2.15	53.30	34.50	540.00	458.00	2.22E+00	1.57E+00
		3.68	2.56	58.20	41.10	591.00	543.00	2.22E+00	1.58E+00
		4.02	3.02	63.00	48.60	644.00	642.00	2.20E+00	1.58E+00
		4.36	3.56	67.30	56.70	694.00	753.00	2.18E+00	1.57E+00
		4.82	4.12	72.40	65.90	746.00	878.00	2.18E+00	1.57E+00
		5.29	4.55	76.80	72.10	791.00	964.00	2.18E+00	1.56E+00
		6.22	5.1	84.70	80.10	871.00	1074.00	2.19E+00	1.56E+00
		6.74	5.6	87.00	86.10	899.00	1170.00	2.18E+00	1.54E+00
		7.32	6.15	89.70	91.50	934.00	1271.00	2.16E+00	1.50E+00

APPENDIX M

Sensitivity Measurement

Sensitivity measurements of polyaniline and polyaniline-10MA/zeolite pellets were carried by using the four point probe at various CO/N_2 concentrations under the pressure guage of 1 atm, 57-67% relative humidity and $30\pm2°C$. The electrical conductivity response of sample was calculated from the difference between the equlibrium conductivity of sample upon exposed to CO and the steady state of final conductivity of sample in N_2.

$$\Delta\sigma = \sigma_{CO} - \sigma_{Final\ N2} \qquad (M.1)$$

However, the addition of zeolite into PANI results in the lowering of the initial conductivity of composite sample. So, the sensitivity is defined as the electrical conductivity response devided by the conductivity itself at the N_2.

$$Sensitivity \quad = \quad \Delta\sigma/\sigma_{N2,final} \qquad (M.1)$$

Table M1 The conductivity response of PANI-1MA exposed to CO-N_2 gas

Sample name	1MA_1	thickness	0.0119 cm	K = 3.8711
Temperature	29 ^{O}C	Humidity	56%	
V_{app}	4.2 V	σ_{air}	2.78E-2 S/cm	

CO (ppm)	σ_{vac}	$\sigma_{exposed}$	$\Delta\sigma$ (S/cm)	$\Delta\sigma/\sigma_{N2}$
1000.0	5.96E-03	6.82E-03	1.07E-03	1.86E-01
500.0	5.74E-03	6.61E-03	8.60E-04	1.50E-01
250.0	5.82E-03	6.44E-03	6.90E-04	1.20E-01
125.0	5.92E-03	6.23E-03	4.80E-04	8.35E-02
62.5	5.86E-03	6.08E-03	3.30E-04	5.74E-02
31.3	5.77E-03	6.00E-03	2.50E-04	4.35E-02
15.6	5.65E-03	5.71E-03	-4.00E-05	-
7.8	5.62E-03	5.82E-03	7.00E-05	1.22E-02
final N_2	5.71E-03	5.75E-03	0.00E+00	-

Sample name	1MA_2	thickness	0.0124 cm	K = 3.9377
Temperature	29 ^{O}C	Humidity	56%	
V_{app}	10.8 V	σ_{air}	2.06E-2 S/cm	

CO (ppm)	σ_{vac}	$\sigma_{exposed}$	$\Delta\sigma$ (S/cm)	$\Delta\sigma/\sigma_{N2}$
1000.0	4.15E-03	4.81E-03	8.60E-04	2.18E-01
500.0	4.02E-03	4.72E-03	7.70E-04	1.95E-01
250.0	4.15E-03	4.69E-03	7.40E-04	1.87E-01
125.0	4.12E-03	4.55E-03	6.00E-04	1.52E-01
62.5	4.10E-03	4.43E-03	4.80E-04	1.22E-01
31.3	4.12E-03	4.26E-03	3.10E-04	7.85E-02
15.6	3.99E-03	4.12E-03	1.70E-04	4.30E-02
7.8	3.88E-03	4.02E-03	7.00E-05	1.77E-02
final N_2	3.83E-03	3.95E-03	0.00E+00	-

Table M2 The conductivity response of PANI-10MA exposed to CO-N_2 gas

Sample name	10MA_1	thickness	0.0109 cm	K = 3.8711
Temperature	28.2 ^{O}C	Humidity	66%	
V_{app}	9.7 V	σ_{air}	1.11 S/cm	

CO (ppm)	σ_{vac}	$\sigma_{exposed}$	$\Delta\sigma$ (S/cm)	$\Delta\sigma/\sigma_{N2}$
1000.0	0.276	0.312	0.045	1.69E-01
500.0	0.275	0.303	0.036	1.35E-01
250.0	0.270	0.290	0.023	8.61E-02
125.0	0.275	0.288	0.021	7.87E-02
62.5	0.272	0.280	0.013	4.87E-02
31.3	0.274	0.278	0.011	4.12E-02
15.6	0.275	0.275	0.008	3.00E-02
7.8	0.268	0.269	0.002	7.49E-03
final N_2	0.265	0.267	0.000	0.00E+00

Sample name	10MA_2	thickness	0.0109 cm	K = 3.9377
Temperature	28.2 ^{O}C	Humidity	66%	
V_{app}	9.8 V	σ_{air}	0.92 S/cm	

CO (ppm)	σ_{vac}	$\sigma_{exposed}$	$\Delta\sigma$ (S/cm)	$\Delta\sigma/\sigma_{N2}$
1000.0	0.208	0.244	0.031	1.46E-01
500.0	0.275	0.237	0.024	1.13E-01
250.0	0.211	0.231	0.018	8.45E-02
125.0	0.212	0.222	0.009	4.23E-02
62.5	0.210	0.217	0.004	1.88E-02
31.3	0.211	0.217	0.004	1.88E-02
15.6	0.209	0.215	0.002	9.39E-03
7.8	0.209	0.213	0.000	0.00E+00
final N_2	0.208	0.213	0.000	0.00E+00

Table M3 The conductivity response of PANI-10MA/10-13X exposed to CO-N_2 gas

Sample name	10MA_10X_1	thickness	0.012 cm	K = 3.8711
Temperature	28.9 ^{O}C	Humidity	53%	
V_{app}	5.4 V	σ_{air}	0.725 S/cm	

CO (ppm)	σ_{vac}	$\sigma_{exposed}$	$\Delta\sigma$ (S/cm)	$\Delta\sigma/\sigma_{N2}$
1000.0	0.043	4.33E-02	0.024	1.19E+00
500.0	0.042	4.23E-02	0.023	1.14E+00
250.0	0.033	3.28E-02	0.013	6.57E-01
125.0	0.029	2.88E-02	0.009	4.55E-01
62.5	0.028	2.78E-02	0.008	4.04E-01
31.3	0.027	2.69E-02	0.007	3.59E-01
15.6	0.025	2.54E-02	0.006	2.83E-01
7.8	0.022	2.42E-02	0.004	2.22E-01
final N_2	0.020	1.98E-02	0.000	0.00E+00

Sample name	10MA_10X_2	thickness	0.0119 cm	K = 3.9377
Temperature	28.9 ^{O}C	Humidity	53%	
V_{app}	5 V	σ_{air}	0.84 S/cm	

CO (ppm)	σ_{vac}	$\sigma_{exposed}$	$\Delta\sigma$ (S/cm)	$\Delta\sigma/\sigma\Delta\sigma/\sigma_{N2}$
1000.0	0.208	0.196	0.059	4.31E-01
500.0	0.275	0.189	0.052	2.63E+00
250.0	0.211	0.175	0.038	1.92E+00
125.0	0.212	0.164	0.027	1.36E+00
62.5	0.210	0.158	0.021	1.06E+00
31.3	0.211	0.151	0.014	7.07E-01
15.6	0.209	0.148	0.014	7.07E-01
7.8	0.209	0.144	0.011	5.56E-01
final N_2	0.208	0.137	0.000	0.00E+00

Table M4 The conductivity response of PANI-10MA/20-13X exposed to CO-N_2 gas

Sample name	10MA_20X_1	thickness	0.0111 cm	K = 3.8711
Temperature	29 ^{O}C	Humidity	66%	
V_{app}	2.8 V	σ_{air}	0.649 S/cm	

CO (ppm)	σ_{vac}	$\sigma_{exposed}$	$\Delta\sigma$ (S/cm)	$\Delta\sigma/\sigma_{N2}$
1000.0	0.092	1.20E-01	0.030	3.38E-01
500.0	0.091	1.17E-01	0.027	3.04E-01
250.0	0.086	1.00E-01	0.010	1.15E-01
125.0	0.085	9.64E-02	0.007	7.47E-02
62.5	0.090	9.63E-02	0.007	7.36E-02
31.3	0.087	9.56E-02	0.006	6.58E-02
15.6	0.089	9.47E-02	0.005	5.57E-02
7.8	0.087	9.17E-02	0.002	2.23E-02
final N_2	0.088	8.97E-02	0.000	0.00E+00

Sample name	10MA_20X_2	thickness	0.012 cm	K = 3.9377
Temperature	29 ^{O}C	Humidity	67%	
V_{app}	5 V	σ_{air}	0.657 S/cm	

CO (ppm)	σ_{vac}	$\sigma_{exposed}$	$\Delta\sigma$ (S/cm)	$\Delta\sigma/\sigma_{N2}$
1000.0	0.133	0.165	0.045	3.75E-01
500.0	0.129	0.140	0.020	1.67E-01
250.0	0.131	0.134	0.014	1.17E-01
125.0	0.121	0.128	0.008	6.67E-02
62.5	0.122	0.123	0.003	2.50E-02
31.3	0.117	0.120	0.000	0.00E+00
15.6	0.113	0.126	0.006	5.00E-02
7.8	0.114	0.12	0.000	0.00E+00
final N_2	0.115	0.120	0.000	0.00E+00

Table M5 The conductivity response of PANI-10MA/40-13X exposed to CO-N_2 gas

Sample name	10MA_40X_1	thickness	0.0111 cm	K = 3.8711
Temperature	29 ^{O}C	Humidity	66%	
V_{app}	2.8 V	σ_{air}	0.0778 S/cm	

CO (ppm)	σ_{vac}	$\sigma_{exposed}$	$\Delta\sigma$ (S/cm)	$\Delta\sigma/\sigma_{N2}$
1000.0	1.06E-02	1.54E-02	9.30E-03	1.52E+00
500.0	8.17E-03	1.52E-02	9.10E-03	1.49E+00
250.0	1.03E-02	1.20E-02	5.90E-03	9.67E-01
125.0	6.36E-03	1.01E-02	4.00E-03	6.56E-01
62.5	6.17E-03	8.83E-03	2.73E-03	4.48E-01
31.3	6.15E-03	8.39E-03	2.29E-03	3.75E-01
15.6	6.02E-03	8.15E-03	2.05E-03	3.36E-01
7.8	5.55E-03	7.24E-03	1.14E-03	1.87E-01
final N_2	5.95E-03	6.10E-03	0.00E+00	0.00E+00

Sample name	10MA_40X_2	thickness	0.012 cm	K = 3.9377
Temperature	28.9	Humidity	67%	
V_{app}	4.1 V	σ_{air}	0.128 S/cm	

CO (ppm)	σ_{vac}	$\sigma_{exposed}$	$\Delta\sigma$ (S/cm)	$\Delta\sigma/\sigma_{N2}$
1000.0	1.30E-02	1.87E-02	5.10E-03	3.75E-01
500.0	1.34E-02	1.75E-02	3.90E-03	2.87E-01
250.0	1.41E-02	1.69E-02	3.30E-03	2.43E-01
125.0	1.45E-02	1.51E-02	1.50E-03	1.10E-01
62.5	1.30E-02	1.43E-02	7.00E-04	5.15E-02
31.3	1.15E-02	1.44E-02	8.00E-04	5.88E-02
15.6	1.19E-02	1.48E-02	8.00E-04	5.88E-02
7.8	1.19E-02	1.38E-02	1.20E-03	8.82E-02
final N_2	1.23E-02	1.36E-02	0.00E+00	0.00E+00

Table M6 The conductivity response of PANI-10MA/10-Y exposed to CO-N_2 gas

Sample name	10MA_10Y_1	thickness	0.0109 cm	K = 3.8711
Temperature	28.5 ^{O}C	Humidity	64%	
V_{app}	5.9 V	σ_{air}	0.976 S/cm	

CO (ppm)	σ_{vac}	$\sigma_{exposed}$	$\Delta\sigma$ (S/cm)	$\Delta\sigma/\sigma_{N2}$
1000.0	0.175	0.228	0.070	4.43E-01
500.0	0.154	0.202	0.044	2.78E-01
250.0	0.163	0.188	0.030	1.90E-01
125.0	0.159	0.191	0.033	2.09E-01
62.5	0.164	0.193	0.035	2.22E-01
31.3	0.164	0.186	0.028	1.77E-01
15.6	0.146	0.181	0.023	1.46E-01
7.8	0.145	0.177	0.019	1.20E-01
final N_2	0.149	0.158	0.000	0.00E+00

Sample name	10MA_10Y_2	thickness	0.0128 cm	K = 3.9377
Temperature	28.5 ^{O}C	Humidity	64%	
V_{app}	4.1 V	σ_{air}	0.788 S/cm	

CO (ppm)	σ_{vac}	$\sigma_{exposed}$	$\Delta\sigma$ (S/cm)	$\Delta\sigma/\sigma_{N2}$
1000	0.201	0.251	0.074	4.18E-01
500	0.185	0.227	0.050	2.82E-01
250	0.189	0.213	0.036	2.03E-01
125	0.178	0.195	0.018	1.02E-01
62.5	0.178	0.201	0.024	1.36E-01
31.25	0.184	0.2	0.023	1.30E-01
15.625	0.166	0.196	0.023	1.30E-01
7.8125	0.162	0.186	0.019	1.07E-01
final N_2	0.163	0.177	0.000	0.00E+00

Table M7 The conductivity response of PANI-10MA/10-MCM41 exposed to CO-N_2 gas

Sample name	10MA_10MCM_1		thickness	0.0107 cm
Temperature	28.5 ^{O}C	Humidity	64%	K = 3.8711
V_{app}	6.5 V	σ_{air}	1.28 S/cm	

CO (ppm)	σ_{vac}	$\sigma_{exposed}$	$\Delta\sigma$ (S/cm)	$\Delta\sigma/\sigma_{N2}$
1000.0	0.342	0.401	0.086	2.73E-01
500.0	0.317	0.355	0.040	1.27E-01
250.0	0.31	0.352	0.037	1.17E-01
125.0	0.302	0.35	0.035	1.11E-01
62.5	0.301	0.339	0.024	7.62E-02
31.3	0.3	0.329	0.014	4.44E-02
15.6	0.302	0.32	0.005	1.59E-02
7.8	0.29	0.319	0.004	1.27E-02
final N_2	0.3	0.315	0.000	0.00E+00

Sample name	10MA_10MCM_2		thickness	0.0128 cm
Temperature	28.5 ^{O}C	Humidity	64%	K = 3.9377
V_{app}	5.9 V	σ_{air}	0.845 S.cm	

CO (ppm)	σ_{vac}	$\sigma_{exposed}$	$\Delta\sigma$ (S/cm)	$\Delta\sigma/\sigma_{N2}$
1000	0.223	0.269	0.051	1.62E-01
500	0.216	0.242	0.024	7.62E-02
250	0.21	0.24	0.022	6.98E-02
125	0.211	0.231	0.013	4.13E-02
62.5	0.205	0.227	0.009	2.86E-02
31.25	0.201	0.236	0.018	5.71E-02
15.625	0.208	0.229	0.011	3.49E-02
7.8125	0.205	0.225	0.007	2.22E-02
final N_2	0.206	0.218	0.000	0.00E+00

CURRICULUM VITAE

Name: Ms. Nataporn Densakulprasert

Date of Birth: January 3, 1981

Nationality: Thai

University Education:

   1997-2001 Bachelor Degree of Science in Chemistry, Faculty of Science, King Monkut's University of Technology Thonburi, Bangkok, Thailand.